

Contourlet Transform for Ocean Remote Sensing Data Fusion

^{1, 2,*}Huimin Lu, ³Nichang Wang and ^{1,*}Seiichi Serikawa

Abstract

Image fusion provides a better view than those provided by any of the individual source images. The aim of multiscale analysis is to find a kind of optimal representation for a high dimensional information expression. In this paper, we consider to use a multiscale analysis method for multisensor and multispectral methods of data fusion. This method is dedicated to fuse multispectral low-resolution remotely sensed images with a more highly resolved panchromatic image. All remotely sensed image coefficients of the low-resolution and high-resolution regions are extracted by contourlet transform (CT). Contourlet transform for a new multi-resolution analysis, whose basis functions are directional edges with a progressively increasing resolution. The advantage of contourlet transform is well adapted to cured-singularities and point-singularities. There are three obvious virtues of this method. Firstly, directional detail coefficients matching image edges is better than that obtained in separable wavelet domain. Secondly, CT prior to curvelet transform uses an ellipse sampling grid to eliminate the difficulty of perfect sampling problem caused by curvelet transform. Thirdly, selection strategy of maximum local energy (MLE) between low-resolution scales is more effective. Experiments in spectral analysis and spatial analysis proved that the MLE is slightly better than the state-of-the-art for multispectral (MS) images fusion.

Keywords: multisensor fusion, ocean, image processing, remote sensing

1. Introduction

The technology of multispectral (MS) data fusion is widely used in many remote sensing and Geographic Information System (GIS). The imaging sensors provide a system with useful information regarding some features of interest in the system environment. However, a single sensor cannot provide a complete view of the scene in many applications [1]. The fused images, if suitably obtained from a set of source sensor images, can provide a better view than that provided by any of

the individual source images. In recent decades, growing interests have focused on the use of multiple sensors to increase the capabilities of intelligent machines and systems. As a result, multi-sensor fusion has become an area of intense research and development in the past few years.

The literature on data fusion in many fields [2,3,4], such as computer vision, machine intelligence and medical imaging, this paper is focused on multi-sensor data fusion in the satellite remote sensing field. Remote sensing techniques [5] have proven to be powerful tools for monitoring the earth's surface. They provide important coverage, mapping and classification of land cover features such as vegetation, soil, water and forests. The volume of remote sensing images continues to grow at an enormous rate due to advances in sensor technology for both high spatial and temporal resolution systems. Consequently, an increasing quantity of image data from satellite sensors have been available, including multi-resolution images, multi-temporal images, multi-spectral bands images and multi-polarization image. Multi-sensor data fusion is a process of combining images, obtained by sensors of different wavelengths to form a composite image to pursue more perfect information from different images than that derived from a single sensor.

Multi-sensor data fusion methods are broadly classified into spatial domain fusion and transform domain fusion. This paper focused on the multi-resolution analysis (MRA) for analyzing remote sensing images in transform domain fusion. A notable application of the satellite remote multi-sensor data fusion is the fusion of multispectral (MS) and panchromatic (Pan) images. Image fusion techniques take advantage of the complementary spatial/spectral resolution characteristics for making spatially enhanced MS observations; it is called band-sharpening. [6]. Band-sharpening is an image fusion methods based on resampling high frequency components of Pan image, combined with the coarse-scale MS data to get the finer scale of the Pan image with minimal introduction of spectral distortions. Some Multi-resolution analysis (MRA) based fusion methods, such as wavelets [7], Laplacian pyramids [8], wedgelets [9], bandelets [10], curvelets [11], contourlets [12], has been recognized as one of the most methods to obtain a fine fusion images at different resolutions.

*Corresponding Author: Seiichi Serikawa

(E-mail: rikukeibin@gmail.com)

¹Dept. of Engineering, Kyushu Institute of Technology, Japan

²Japan Society for the Promotion of Science, Japan

³Yangzhou Radio Management Monitoring Station, China

The pyramid method firstly constructs the input image pyramid, and then takes some feature selection approach to form the fusion value pyramid. By the inverter of the pyramid, the pyramid of images can be reconstructed to produce fusion images. This method is relatively simple, but it also has some drawbacks. Therefore, discrete wavelet transform (DWT) method is proposed to improve the multi-resolution problem. Discrete wavelet transform (DWT) can be decomposed into a series of sub-band images with different resolution, frequency and direction characteristics. The spectral characteristics and spatial characteristics of image are completely separated. to get the different resolution image fusion. But because of limited directional of wavelet, it cannot express line- or curve-singularities in two- or higher dimensional signals. Therefore, some other excellent multi-resolution analysis (MRA) methods are proposed in recent years to improve the drawbacks of wavelets. Minh N. Do and Martin Vetterli proposed contourlet transform [12] in 2002. That develops a transform in the continuous domain first, and then discretizes for sampled data.

In this paper, we propose an image fusion method for Pan-sharpening of very low resolution MS images, which operates in the contourlet transform (CT). We apply maximum local energy method (MLE) and sum-modified Laplacian (SML) in this work. Particularly, for remote images fusion, we selected the low-resolution coefficients by maximum local energy (MLE) method, and introduced sum modified Laplacian (SML) [14] to calculate the high-resolution coefficients. In Section II, we briefly introduce contourlet in this work. As a solution, we propose in Section III a new fusion method, named maximum local energy method. Numerical experiments are presented in Section IV to confirm our method. We conclude the paper in Section V.

2. Contourlet Transform

Because of the frequency division in Figure 1(b) is obtained by ideal filters. When non-ideal filters are combined with Laplacian pyramid, we show a more realistic illustration of one of the directional filters from the direction filter banks in Figure 2(a). If the directional filter must first be upsampled by 2 along each dimension as shown in Figure 2(b). Because of the upsampling, the aliasing components are folded towards the low-pass regions and concentrated mostly along two lines $\omega_2 = \pm\pi/2$. Combining the upsampled DFB was shown in Figure 2(c). In Figure 2(d), we can see the resulting of contourlet subband. The CT is not localized in frequency, with substantial amount of aliasing components outside the desired trapezoid-shaped support.

Do and Vetterli [12] proposed an efficient directional multi-resolution image representation called contourlet transform in 2002. Contourlet is a “true” two-dimensional transform that can capture the intrinsic geometrical structure, and it has been applied to several tasks in image processing. Contourlet transform (CT) better represents the salient features of the image such as, edges, lines, curves, and contours, than wavelet transform because of its anisotropy and directionality. Two steps are involved in CT, subband decomposition and the directional transform. CT uses the Laplacian pyramid (LP) to decompose the image in multiscale form before adopting the directional filter banks (DFB) to decompose the high frequency coefficients and obtain details with different directions of the directional subband. CT accurately expresses directions. We can see that the Laplacian pyramid shown in the diagram is a simplified version of its actual implementation as shown in Figure 1.

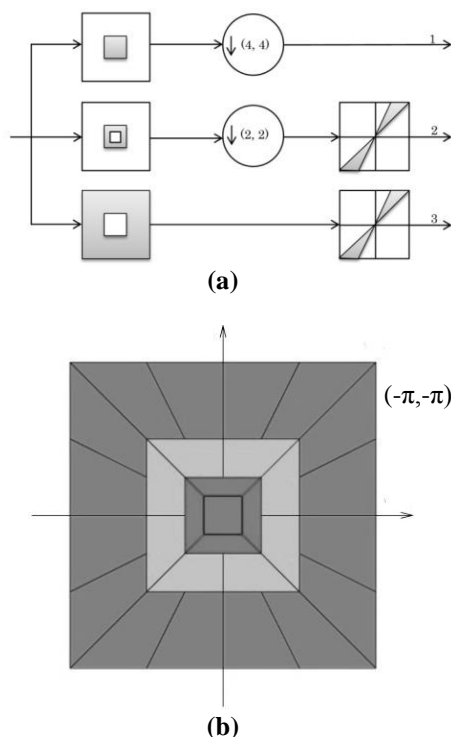


Figure 1: The original contourlet transform. (a) The equivalent parallel form of original block diagram. (b) Resulting frequency division.

The frequency division in Figure 1(b) is obtained by ideal filters. When non-ideal filters are combined with Laplacian pyramid, we show a more realistic illustration of one of the directional filters from the direction filter banks in Figure 2(a). If the directional filter must first be upsampled by 2 along each dimension as shown in Figure 2(b). Because of the upsampling, the aliasing components are folded towards the low-pass regions and concentrated mostly along two lines $\omega_2 = \pm\pi/2$. Combining the upsampled DFB was shown in Figure 2(c). In Figure 2(d), we can see the resulting of contourlet subband. The CT is not localized in frequency, with substantial amount of aliasing components outside the desired trapezoid-shaped support.

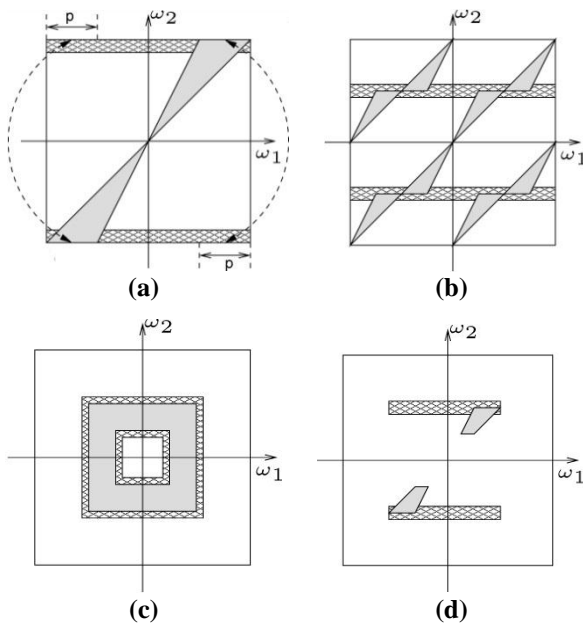


Figure 2: Illustration of the frequency domain aliasing problem of the contourlet transforms. (a) One directional filter (b) The directional filter after being upsampled by 2 along each dimension (c) A bandpass filter from the Laplacian pyramid (d) The resulting contourlet subband

3. Fusion Rules

In this paper, we propose a new fusion model. Figure 3 shows the flowchart of a SFLCT-based scheme suitable for fusion of MS and Pan data, whose scale is an integer $p=4$. Let $f^{(p)}(i,j)$ be the dataset constituted by a single Pan image with a smaller scale, and size being $M_p \times N_p$. Let $\{f^{(l)}(i,j), l=1, \dots, L\}$ be the dataset made up of the L bands of an MS image. The enhancement of each band to yield the spatial resolution of Pan image is synthesized from the layer c_1 (middle layer) and c_2 (high layer) of the M-SFLCT.

Firstly, obtain $\{\hat{f}^{(l)}(i,j), l=1, \dots, L\}$ of MS bands with the same spatial resolution as Pan image. Each of l -th band $\{\hat{f}^{(l)}(i,j)\}$ of the new MS bands $\{\hat{f}^{(l)}(i,j), l=1, \dots, L\}$ are preliminarily interpolated by scale p to match the scale of the Pan image. The constitution of low-resolution components of Pan image and l -th band MS image are processed by maximum local energy (MLE) rule. In the level i_l of resolved Pan image and l -th band MS image, the local energy components are obtained by a 3×3 sliding window and then output the maximum component of two source images. In the layers c_1 (middle layer) and c_2 (high layer), we use a spatial domain measurement [22], the sum modified Laplacian (SML), as a high-resolution fusion rule. The modified Laplacian takes the absolute values of the second derivatives in the Laplacian to avoid the cancellation of the second derivatives in the horizontal and vertical directions that have opposite signs. At the same time, MLE rule can adapt to adjust SML rule. Finally, by means of the inverse CT, two images of zero-mean spatial edges and textures are added to the corresponding

frames. The final Pan-sharpened MS image $\{\tilde{f}^{(l)}(i,j), l=1, \dots, L\}$ is received by summing the approximations and enhanced detail frames of each band in CT synthesis.

This paper takes the maximum local energy (MLE) [10] as a measurement. Due to the incompleteness of multi-scale decomposition, image details are still retained in the low frequency. Therefore, some edge filters are proposed to get a good result. But because of the edge filter coefficients distribute as non-Gaussian distribution, combining with local energy can solve this problem well. Select the maximum energy of two low layer i_l images as output. Due to the partial human visual perception characteristics and the relationship of decomposition about local correlation coefficients, the statistical characteristics of neighbors should be considered. Therefore, the statistic algorithm is based on the 3×3 sliding window. The algorithm is described as follows:

$$LE_{\xi}(i, j) = \sum_{i \in M, j \in N} p(i+i', j+j') \bullet f_{\xi}^{(0)2}(i+i', j+j') \quad (1)$$

Where p is the local filtering operator. M, N is the scope of a local window. $\xi \in A$ or B (A, B is the window for scanning two images). $f_{\xi}^{(0)}(i, j)$ is low frequency coefficients.

Maximum Local Contourlet Energy is

$$\begin{aligned} MaxLCE_{\xi}^{l,k}(i, j) &= E_1 * f_{\xi}^{(0)2}(i, j) + E_2 * f_{\xi}^{(0)2}(i, j) \\ &+ \dots + E_K * f_{\xi}^{(0)2}(i, j). \end{aligned} \quad (2)$$

Where E_1, E_2, \dots, E_{K-1} and E_K are the filter operators in K different directions. l is the scale layer.

$$E_1 = \begin{bmatrix} -1 & -1 & -1 \\ 2 & 2 & 2 \\ -1 & -1 & -1 \end{bmatrix}, E_2 = \begin{bmatrix} -1 & 2 & -1 \\ -1 & 2 & -1 \\ -1 & 2 & -1 \end{bmatrix}, E_3 = \begin{bmatrix} -1 & 0 & -1 \\ 0 & 4 & 0 \\ -1 & 0 & -1 \end{bmatrix} \quad (3)$$

We adopt summing modified Laplacian as a rule to fuse high-resolution images. Suppose $I_A^{l,k}(i,j)$, $I_B^{l,k}(i,j)$ and $I_F^{l,k}(i,j)$ denote the coefficients of source images and fused images. The proposed MLE-based fusion rule can be described as follows

$$I_F^{l,k}(i,j) = \begin{cases} I_A^{l,k}(i,j), & \text{if } : LCE_A^{l,k}(i,j) \geq LCE_B^{l,k}(i,j) \\ I_B^{l,k}(i,j), & \text{if } : LCE_A^{l,k}(i,j) < LCE_B^{l,k}(i,j) \end{cases} \quad (4)$$

The defined modified Laplacian (ML) [14] is

$$\nabla_{ML}^2 f(x,y) = |2f(x,y) - f(x-\text{step},y) - f(x+\text{step},y)| + |2f(x,y) - f(x,y-\text{step}) - f(x,y+\text{step})| \quad (5)$$

In this paper "step" always equals to 1.

$$SML_x^{l,k}(i,j) = \sum_{i=-M}^M \sum_{j=-N}^N \nabla_{ML}^2 f(i+p, j+q) \quad (6)$$

$$\text{for } \nabla_{ML}^2 f(i,j) \geq T$$

Where l, k are, respectively, the scale and the direction of transform. $x \in A$ or B is, respectively, the source images. T is a discrimination threshold value. M, N determine the window with size of $(2M+1) \times (2N+1)$.

Suppose $C_A^{l,k}(i,j)$, $C_B^{l,k}(i,j)$ and $C_F^{l,k}(i,j)$ denote the coefficients of source images and fused images. The proposed SML-based fusion rule can be described as follows:

$$C_F^{l,k}(i,j) = \begin{cases} C_A^{l,k}(i,j), & \text{if } : SML_A^{l,k}(i,j) \geq SML_B^{l,k}(i,j) \\ C_B^{l,k}(i,j), & \text{if } : SML_A^{l,k}(i,j) < SML_B^{l,k}(i,j) \end{cases} \quad (7)$$

4. Experiment and Analysis

The proposed modified sharp frequency localized contourlet transform-based fusion has been assessed on three very high-resolution image datasets collected by SPOT, IKONOS, Landsat and QuickBird. The data set displays the Ujong Kulon National Park by QuickBird-2 satellite, in Indonesia. Square area of scene size is 16.5×16.5 km. Pixel resolutions of MS image and Pan image are 2.44-2.88m, and 0.61-0.72 m, respectively. In the next subsection, some quality assessment indexes are introduced. And latter, present the experimental results, and discuss the behavior of the different fusion methods.

The quality assessment of Pan-sharpened MS images is a difficult task. Fidelity assessment to the reference requires computation of several indexes. These indexes are on spectral consistency, spatial consistency or both together. Spectral consistency assumes that pansharpened data have increased spatial resolution with spectral properties of the original image. We conducted some quantitative analysis, mainly from the perspective of mathematical statistics aspect, and the image's statistical parameters are calculated, which include Peak Signal to Noise Ratio (PSNR), mean squared error (MSE), fusion quality index (Q), weighted fusion quality index (QW), edge-dependent fusion quality index (QE) [17], Structural SIMilarity (SSIM) [18], Multi-scale Structural SIMilarity (MS-SSIM) [19,20] and band-to-band correlation coefficients (CCs) [21] et al.. Spatial consistency assumes that a high spatial quality merged image is to incorporate the spatial detail features present in the panchromatic image with the missing in the initial multispectral image, such as phase congruency (PC) [30].

Let x_i and y_i be the i -th pixel in the original image \mathbf{x} and the distorted image \mathbf{y} , respectively. The MSE and $PSNR$ between the two images are given by

$$MSE = \frac{1}{N} \sum_{i=1}^N (x_i - y_i)^2, \quad (8)$$

$$PSNR = 10 \log_{10} \left(\frac{L^2}{MSE} \right) \quad (9)$$

In [18], the authors use a sliding window, from the top-left of the two images A, B . The sliding window is with a fixed size. For each window w , the local quality index $Q_0(A, B | w)$ is computed for the values $A(i, j)$ and $B(i, j)$, where pixels (i, j) lies in the sliding window w .

$$Q_0(A, B) = \frac{1}{|W|} \sum_{w \in W} Q_0(A, B | w), \quad (10)$$

Where W is the family of all windows and $|W|$ is the cardinality of W . In practice, the Q_0 index also defined as

$$Q_0(A, B) = \frac{\sigma_{AB}}{\sigma_A \cdot \sigma_B} \cdot \frac{2\bar{A} \cdot \bar{B}}{[(\bar{A})^2 + (\bar{B})^2]} \cdot \frac{2\sigma_A \cdot \sigma_B}{(\sigma_A^2 + \sigma_B^2)} \quad (11)$$

Where σ_{AB} denotes the covariance between A and B , \bar{A} and \bar{B} are the means, and σ_A^2 and σ_B^2 are the variances of A and B , respectively.

Piella et al. [17] redefined the useful quality index Q_0 as $Q(A, B, F)$ for image fusion assessment. Here A, B are two input images, and F is the fused image. They are denoted by $s(A|w)$ some saliency of image A in window w . This index may depend on contrast, sharpness, or entropy. The local weight $\lambda(w)$ is defined as

$$\lambda(w) = \frac{s(A|w)}{s(A|w) + s(B|w)} \quad (12)$$

Where $s(A|w)$ and $s(B|w)$ are the local saliencies of input images A and B , $\lambda \in [0, 1]$. The fusion quality index $Q(A, B, F)$ as

$$Q(A, B, F) = \frac{1}{|W|} \sum_{w \in W} (\lambda(w)Q_0(A, F|w) + (1 - \lambda(w))Q_0(B, F|w)) \quad (13)$$

They also define the overall saliency of a window as $C(w) = \max(s(A|w), s(B|w))$. The weighted fusion quality index is then defined as

$$Q_W(A, B, F) = \sum_{w \in W} c(w) (\lambda(w)Q_0(A, F|w) + (1 - \lambda(w))Q_0(B, F|w)) \quad (14)$$

Where $c(w) = C(w) / (\sum_{w' \in W} C(w'))$. Using edge images

A', B', F' inside original images A, B , and F , $Q_W(A, B, F)$ and $Q_W(A', B', F')$ are combined into an edge-dependent fusion quality index by

$$Q_E(A, B, F) = Q_W(A, B, F) \cdot Q_W(A', B', F')^\alpha \quad (15)$$

Where α is a parameter that expresses the contribution of the edge images compared to the original images.

In [18], a multi-scale SSIM method for image quality assessment is proposed. Input to signal A and B , let μ_A, σ_A and σ_{AB} be, respectively, as the mean of A , the variance of A , and the covariance of A and B . The parameters of relative importance α, β, γ are equal to 1. The SSIM is given as follows:

$$SSIM(x, y) = \frac{(2\mu_A\mu_B + C_1)(2\sigma_{AB} + C_2)}{(\mu_A^2 + \mu_B^2 + C_1)(\mu_A^2 + \mu_B^2 + C_2)} \quad (16)$$

Where C_1, C_2 are small constants. The overall multi-scale SSIM (MS-SSIM) evaluation at the j -th scale with Scale M is obtained by

$$MS-SSIM(A, B) = [l_M(A, B)]^{\alpha M} \cdot \prod_{j=1}^M [c_j(A, B)]^{\beta j} [s_j(A, B)]^{\gamma j} \quad (17)$$

Where $l(A, B)$, $c(A, B)$, $s(A, B)$ are the luminance, contrast and structure comparison measures, respectively.

An image quality index for MS images with four spectral bands was proposed [21] for assessing Pan-sharpening methods. The quality index Q4 is a generalization to 4-band images of the Q index. The Q4 is defined as

$$Q_{4,N} = \left\{ \frac{\sigma_{AB}}{\sigma_A \cdot \sigma_B} \cdot \frac{2\sigma_A \cdot \sigma_B}{\sigma_A^2 + \sigma_B^2} \cdot \frac{2|\bar{A}| \cdot |\bar{B}|}{|\bar{A}|^2 + |\bar{B}|^2} \right\}_{N \times N} \quad (18)$$

Where the parameters are referred in the above. The first is the modulus of the hypercomplex correlation coefficients (CCs) between the two spectral pixel vectors, and is sensitive both to loss of correlation and to spectral distortion between the two MS data sets. The second and third terms, respectively, measure contrast changes and mean bias on all bands simultaneously. All statistics are calculated as averages on $N \times N$ blocks, where $N = 32$. Eventually, Q4 is averaged over the whole image to yield the global score index. The highest value of Q4 is attained if and only if the test MS image is equal to the reference, 1; the lowest value is 0.

Wald et al [23] proposed the relative dimensionless global error in synthesis (ERGAS) in 1997. It is given by

$$ERGAS = 100 \frac{h}{l} \sqrt{\frac{1}{K} \sum_{k=1}^K \left(\frac{RMSE(k)}{\mu(k)} \right)^2} \quad (19)$$

Where h/l is the high/low resolution images ratio (here, is the ratio between pixel sizes of Pan and MS). $\mu(k)$ is the mean (average) of the k -th band, and K is the number of bands.

Phase congruency is used for feature extraction on an image in spatial consistency analysis. Phase congruency at point x is defined as follows,

$$PC(x) = \frac{\sum_o \sum_s W_o(x) [FA_{so}(x) \Delta \Phi_{so}(x) - T_o]}{\sum_o \sum_s FA_{so}(x) + \varepsilon} \quad (20)$$

Where FA_{so} is the amplitude of the component in Fourier series expansion, $\Delta \Phi_{so}$ is the phase deviation function, W_o is the PC weighting function, o is the index over orientation, s is the index over scale, T_o is the noise compensation term, ε is the term added to prevent division by zero, and $\lfloor \rfloor$ means that the enclosed quantity is permitted to be non-negative.

Table 1 shows the 0.72m QuickBird-2 Pan image and 2.88m QuickBird-2 MS image fusion qualities. For $h/l=1/4$ QuickBird-2 Pan image and MS image fusion, WT, M-SFLCT and GS yield average CCs more than that of other methods. However, CCs between fused MS and reference originals may be valid detectors of fusion artifacts, and the parameters with global distortion of pixel vectors are also adopted in this work, such as Q4, ERGAS, MS-SSIM,

giving a more comprehensive measure of quality. From Table 3 we can see that the Q4, SSIM, and MS-SSIM values of M-SFLCT are higher than others. M-SFLCT has global scores better than the other methods, followed by CT, GS and WT methods. The WT, CT and M-SFLCT are obviously better than the other methods at PC assessment analysis. From Figure 4, the details of the M-SFLCT and CT fused images are obvious clearly than the other methods.

Table 1: The average quality assessments of QuickBird-2 Pan image and MS image fusion.

	IHS	PCA	Brovoy	GS	WT	CT
CCs	0.7346	0.7340	0.7279	0.9200	0.7575	0.7133
$Q4_N$	0.6355	0.6728	0.3397	0.6646	0.7462	0.6816
ERGAS	18.511	17.403	24.085	17.100	18.878	22.214
SSIM	0.5224	0.5965	0.3602	0.4509	0.7369	0.7015
MS-SSIM	0.6960	0.7146	0.5758	0.8028	0.8277	0.8000
PC	0.4844	0.4851	0.4763	0.6213	0.8211	0.8381

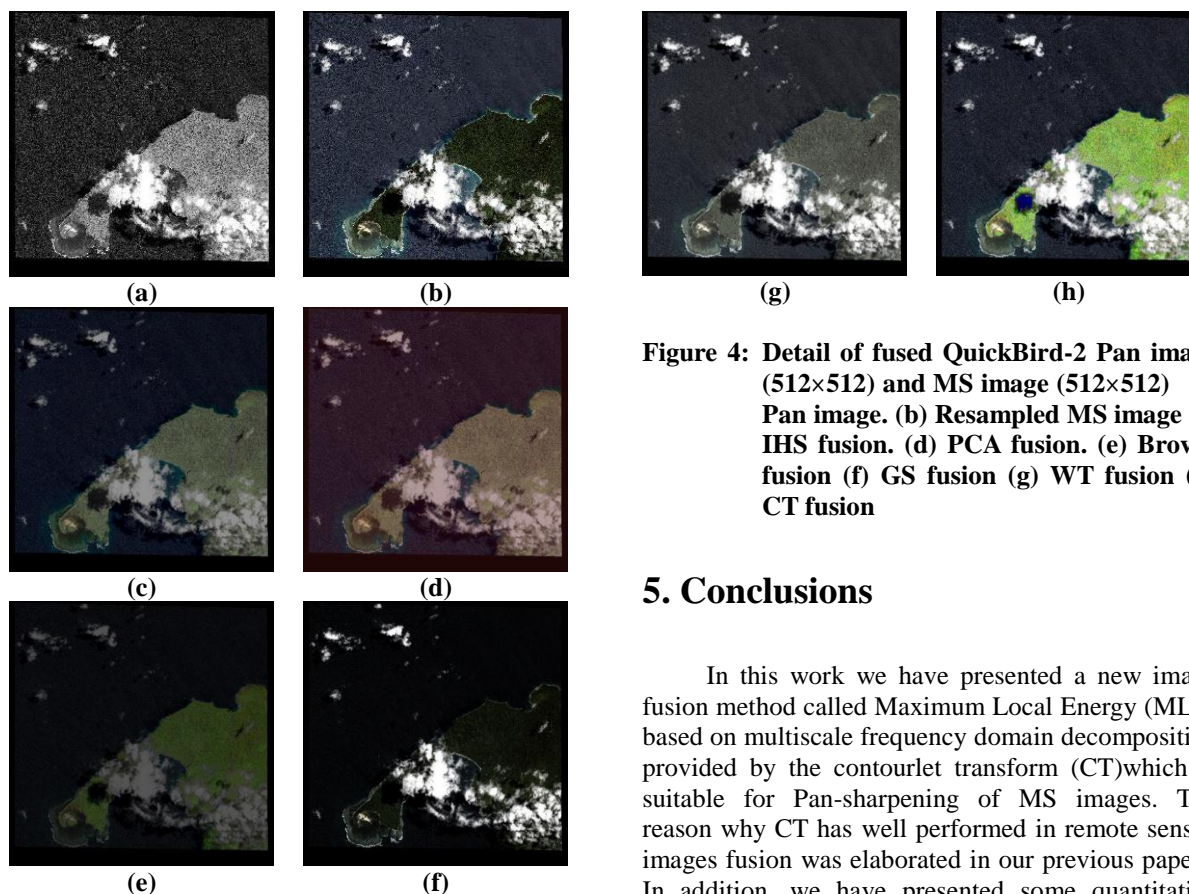


Figure 4: Detail of fused QuickBird-2 Pan image (512×512) and MS image (512×512) (a) Pan image. (b) Resampled MS image (c) IHS fusion. (d) PCA fusion. (e) Brovay fusion (f) GS fusion (g) WT fusion (h) CT fusion

5. Conclusions

In this work we have presented a new image fusion method called Maximum Local Energy (MLE), based on multiscale frequency domain decomposition provided by the contourlet transform (CT) which is suitable for Pan-sharpening of MS images. The reason why CT has well performed in remote sensed images fusion was elaborated in our previous papers. In addition, we have presented some quantitative measurements of Pan-sharpening performance that measure both spatial and spectral quality of the resulting Pan-sharpened images. The results are certified that MLE algorithm is the strongest spatiality of the seven methods while maintaining a reasonable color balance. Another advantage of

performing fusion in the modified sharp frequency localized transform is that it keeps the high-resolution detail coefficients of MS bands and of the Pan image very well. From the results, we also find that it is very suitable for single satellite sensors images fusion.

Acknowledgment

This work was partially supported by Research Found of Japan Society for the Promotion of Science (No.25J10713). The authors wish to thank Japan Aerospace Exploration Agency (JAXA) and University of Maryland Global Land Cover Facility (GLCF) for offering sensed images. The authors also gratefully acknowledge the helpful comments and suggestions of the reviewers.

References

- [1]. Serikawa, S., Gotoh, M., Miyauchi, M. and Shimomura, T., A Method for Signal Supplementation for Sensor Fusion. *Trans. on Inst. Elec. Eng. of Japan*, 2004, 124, 152-153.
- [2]. Lu, H.M., Hu, X.L., Zhang, L.F., Serikawa, S., Local Energy based Image Fusion in Sharp Frequency Localized Contourlet Transform. *J.Comp. Info. Sys.*, 2010, 6, 3997-4005.
- [3]. Howard A., Seraji, H., Multi-sensor Terrain Classification for Safe Spacecraft Landing. *IEEE Trans. on Aero. & Elec. Sys.*, 2004, 40, 1122-1131.
- [4]. Megalooikonomou, V., Kontos, D., Medical Data Fusion for Telemedicine. *IEEE Trans. on Eng. Med. Biol. Mag.*, 2007, 26, 36-42.
- [5]. Pohl, C., and Van Genderen, J.L., Multisensor Image Fusion in Remote Sensing: Concepts, Methods and Applications. *Int.J.Remote Sensing.*, 1998, 19, 823-854.
- [6]. Kumar, A.S., Kartikeyan, B., Majumdar, K.L., Band Sharpening of IRS-multispectral Imagery by Cubic Spline Wavelets. *Int. J. Remote Sensing*, 2000, 21, 581-594.
- [7]. Nunez, J., Otazu, X., Fors, O., Prades, A., Pala, V., Ariol, R., Multiresolution-based Image Fusion with Additive Wavelet Decomposition. *IEEE Trans. on Geo. & Remote Sensing*, 1999, 37, 1204-1211.
- [8]. Aiazzi, B., Alparone, L., Baronti, S., Lotti, F., Lossless Image Compression by Quantization Feedback in a Content-driven Enhanced Laplacian Pyramid. *IEEE Trans. on Image Proc.*, 1997, 6, 831-843.
- [9]. Mahyari, A.G., Yazdi, M., Panchromatic and Multispectral Image Fusion Based on Maximization of Both Spectral and Spatial Similarities. *IEEE Trans. on Geo. & Remote Sensing.*, 2011, 49, 1976-1985.
- [10]. Maalouf, A., Carre, P., Augereau, B., Fernandez-Maloigne, C., A Bandelet-Based Inpainting Technique for Clouds Removal From Remotely Sensed Images. *IEEE Trans. on Geo. & Remote Sensing*, 2009, 47, 2363-2371.
- [11]. Nencini, F., Garzelli, A., Baronti, S., Alparone, L., Remote Sensing Image Fusion Using the Curvelet Transform. *Info. Fusion.*, 2007, 8, 143-156.
- [12]. Donoho, M.N., and Vetterli, M., The Contourlet Transform: An Efficient Directional Multiresolution Image Representation, *IEEE Trans. Image Proc.*, 2005, 14, 1-16.
- [13]. Lu, Y., and Donoho, M.N., A New Contourlet Transform with Sharp Frequency Localization, *International Conference on Image Processing*, IEEE, 2006; pp.1629-1632.
- [14]. Stanciu, S.G., Dragulinescu, M., Stanciu, G.A., Sum-Modified-Laplacian Fusion Methods Experimented on Image Stacks of Photonic Quantum Ring Laser Devices Collected By Confocal Scanning Laser Microscopy. *U.P.B. Sci. Bull., Series A*, 2011, 73, 139-146.
- [15]. Cunha, A.L., Zhou, J., Donoho, M.N., The Nonsampled Contourlet Transform: Theory, Design and Applications. *IEEE Trans. on Image. Proc.*, 2006, 15, 3089-3101.
- [16]. Lu, H.M. Nakashima, S., Li, Y.J., Zhang, L.F., Yang, S.Y., Serikawa, S., An Improved Method for CT/MRI Image Fusion on Bandelelets Transform Domain. *Appl. Mech. & Mat.*, 2012, 103, 700-704.
- [17]. Piella, G., Heijmans, H., A New Quality Metric for Image Fusion. in: *IEEE Inter. Conf. on Image Proc.* 2003; Volume 2, pp. 173-176.
- [18]. Wang, Z., Li, Q., A Universal Image Quality Index. *IEEE Trans. on Sign. Proc. Lett.*, 2002, 9, 81-84.
- [19]. Wang, Z., Simoncelli, E.P., Bovik, A. C., Image Quality Assessment: From Error Visibility to Structural Similarity. *IEEE Trans on Image Proc.*, 2004, 13, 600-612.
- [20]. Wang, Z., Li, Q., Information Content Weighting for Perceptual Image Quality Assessment. *IEEE Trans on Image Proc.*, 2011, 20, 1185-1198.

- [21]. Alparone, L., Baronti, S., Garzelli, A., Nencini, F., A Global Quality Measurement of Pan-Sharpned Multispectral Imagery, *IEEE Trans. on Geo. & Remote Sens. Lett.*, 2004, 1, 313-317.
- [22]. Huang, W., Jing, Z., Evaluation of Focus Measures in Multi-focus Image Fusion. *Pattern Recogn. Lett.*, 2007, 28, 493-500.
- [23]. Wald, L., Ranchin, T., Mangolini, M., Fusion of Satellite Images of Different Spatial Resolutions: Assessing the Quality of Resulting Images. *Photogramm. Eng. Remote Sens.*, 1997, 63, 691-699.
- [24]. Nunez, J., Otazu, X., Fors, O., Prades, A., Arbiol, R., Multiresolution-based Image Fusion with Additive Wavelet Decomposition. *IEEE Trans. on Geo. & Remote Sens.*, 1999, 37, 1204-1211.
- [25]. Maria, G.A., Jose, L.S., Raquel, G.C., Rafael, G., Fusion of Multispectral and Panchromatic Images Using Improved HIS and PCA Mergers Based on Wavelet Decomposition. *IEEE Trans. on Geo. & Remote Sens.*, 2004, 42, 1291-1299.
- [26]. Teming, T., Yuhchi, L., Chienping, C., Pingsheng, H., Adjustable Intensity-hue-saturation and Brovey Transform Fusion Technique for IKONOS/QuickBird Imagery. *Opti. Eng.*, 2005, 44, 116201-1-10.
- [27]. Aiazzi, B., Baronti, S., Selva, M., Improving Component Substitution Pansharpening Through Multivariate Regression of MS+Pan Data. *IEEE Trans. on Geo. & Remote Sens.*, 2007, 45, 3230-3239.
- [28]. Yocky, D., Image Merging and Data Fusion by Means of the Discrete Two-dimensional Wavelet Transform. *J. of Opti. Soci. of Amer.* 1995, 12, 1834-1841.
- [29]. Alparone, L., Baronti, S., Garzelli, A., Nencini, F., The Curvelet Transform for Fusion of Very-high Resolution Multi-spectral and Panchromatic Image. in: *Proc. of 25th EARSeL Sym. Millpress Science Publishers, The Netherlands, 2006.*
- [30]. Kovesi, P., Image Features From Phase Congruency. *J. Comp. Vis. Res.*, 1999, 1, 2-26.
- [31]. Lu, H.M., Zhang, L.F., Serikawa, S., Maximum local energy: an effective approach for image fusion in beyond wavelet transform domain, *Computers & Mathematics with Applications*, 2012, 64(5), 21-26.
- [32]. Serikawa S., Lu, H.M., Underwater Image Dehazing Using Joint Trilateral Filter, *Computers and Electrical Engineering*, 2014, 40(1), 41-50.